

# Structure-Based Enzyme Tailoring of 5-Hydroxymethylfurfural Oxidase

Willem P. Dijkman,<sup>†,§</sup> Claudia Binda,<sup>‡,§</sup> Marco W. Fraaije,<sup>\*,†</sup> and Andrea Mattevi<sup>\*,‡</sup>

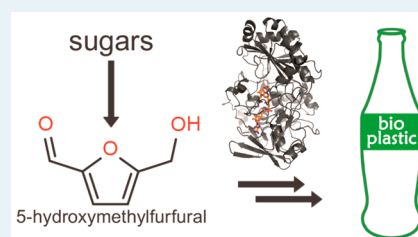
<sup>†</sup>Molecular Enzymology Group, Groningen Biomolecular Sciences and Biotechnology Institute, University of Groningen, Nijenborgh 4, 9747 AG Groningen, The Netherlands

<sup>‡</sup>Department of Biology and Biotechnology, University of Pavia, via Ferrata 1, 27100 Pavia, Italy

## S Supporting Information

**ABSTRACT:** 5-Hydroxymethylfurfural oxidase (HMFO) is a flavin-dependent enzyme that catalyzes the oxidation of many aldehydes, primary alcohols, and thiols. The three-step conversion of 5-hydroxymethylfurfural to 2,5-furandicarboxylic acid is relevant for the industrial production of biobased polymers. The remarkable wide substrate scope of HMFO contrasts with the enzyme's precision in positioning the substrate to perform catalysis. We have solved the crystal structure of HMFO at 1.6 Å resolution, which guided mutagenesis experiments to probe the role of the active-site residues in catalysis. Mutations targeting two active-site residues generated engineered forms of HMFO with promising catalytic features, namely enantioselective activities on secondary alcohols and improved 2,5-furandicarboxylic acid yields.

**KEYWORDS:** 5-hydroxymethylfurfural oxidase, enzyme, 2,5-furandicarboxylic acid, biocatalysis, protein engineering, crystal structure



## INTRODUCTION

The enzyme 5-hydroxymethylfurfural oxidase from *Methylovorus* sp. strain MP688 (HMFO, EC 1.1.3.47) catalyzes the oxidation of 5-hydroxymethylfurfural (**1**) to 2,5-furandicarboxylic acid (**4**);<sup>1</sup> the latter can be esterified to form polymers with a wide variety of applications.<sup>2,3</sup> Because 5-hydroxymethylfurfural (**1**) can be derived from sugars, the enzyme is of particular interest for the production of biobased plastic materials in an environmentally friendly industrial process. The overall reaction consists of three oxidation steps, and HMFO can perform all these steps, as depicted in Scheme 1.<sup>4</sup> The alcohol group of 5-hydroxymethylfurfural (**1**) is first oxidized to the corresponding aldehyde to generate furan-2,5-dicarbaldehyde (**2**).<sup>4</sup> This compound undergoes spontaneous hydration to the *gem*-diol, which is oxidized by the enzyme to 5-formyl-2-furancarboxylic acid (**3**). Finally, also this monocarboxylic intermediate product is released, nonenzymatically hydrated, and oxidized by HMFO to the dicarboxylic reaction product.<sup>4</sup> Importantly, the poor activity of HMFO toward 5-formyl-2-furancarboxylic acid (**3**) is limiting the efficiency of the overall process. Increasing the activity toward 5-formyl-2-furancarboxylic acid (**3**) is addressed in this study.

HMFO is a member of the glucose-methanol-choline (GMC) family of oxidoreductases.<sup>1</sup> HMFO, like other members of this enzyme family, relies on the presence of the flavin adenine dinucleotide (FAD) cofactor as a prosthetic group and an active site histidine (H467 in HMFO) serving as base. This residue, which is conserved in all GMC enzymes,<sup>5–10</sup> initiates the reaction by removing the proton from the alcohol group of the substrate. The second step, taking place simultaneously with or after proton abstraction,<sup>11–13</sup> is the hydride transfer from the  $\alpha$ -carbon of the substrate to the FAD

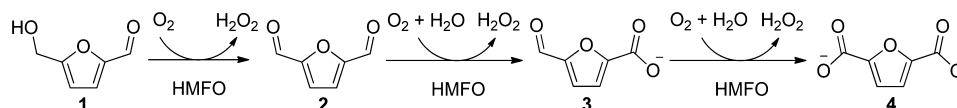
NS, thereby completing the oxidation reaction. This results in the reduced flavin, which is reoxidized by molecular oxygen, yielding hydrogen peroxide as a byproduct (Scheme 1). The active site histidine is crucial for catalysis, functioning as the main anchoring element for the alcohol group of the substrate.<sup>1</sup> The nature of this alcohol group is very important, as only primary alcohols, primary thiols, and hydrated aldehydes are oxidized by HMFO.<sup>14</sup> Secondary alcohols are not converted, indicating that the enzyme is very specific concerning the substrate type.<sup>1</sup> On the other hand, HMFO is strikingly promiscuous concerning the side chain next to the alcohol group. Most (but not all) of the identified substrates are aromatic, including furanic, phenylic, and cinnamyl alcohols. Ring substituents with different sizes, polarities, and charges are allowed in the active site of HMFO, on both the para and meta positions relative to the alcohol.<sup>1</sup>

To investigate how this biocatalyst can be so precise in accepting hydrated aldehydes, primary alcohols, and thiols and yet be so promiscuous concerning the rest of the substrate, we solved the HMFO crystal structure. The three-dimensional model provides the framework for protein engineering studies aimed at the generation of variants with interesting and improved biocatalytic properties. In particular, several HMFO mutants were designed and produced which display higher activities toward 5-formyl-2-furancarboxylic acid (**3**), thereby improving the enzymatic formation of 2,5-furandicarboxylic acid (**4**) from 5-hydroxymethylfurfural (**1**). In addition, mutant enzymes were designed which can enantioselectively convert

Received: January 8, 2015

Revised: February 6, 2015

Published: February 9, 2015

Scheme 1. Oxidation of 5-Hydroxymethylfurfural (1) to 2,5-Furandicarboxylic Acid (4) by HMFO<sup>a</sup>

<sup>a</sup>Conversion of 1 to 4 is initiated by oxidation of the alcohol group of 1, resulting in furan-2,5-dicarbaldehyde (2). The hydrated form of 2 is converted to 5-formyl-2-furancarboxylic acid (3). The last step is the oxidation of the hydrated form of 3, yielding 4.

secondary alcohols, an activity not found in the wild type enzyme.

## MATERIALS AND METHODS

**Purification of HMFO.** For kinetic and spectral analysis, HMFO and its mutants were expressed as a N-terminal SUMO fusion protein in *Escherichia coli* BL21 (DE3) and purified using affinity chromatography as described before.<sup>1</sup> For structural characterization similar procedures were used in the first steps of HMFO purification, including affinity purification, which was performed on a 5 mL HisTrap HP column using an Äkta Purifier system (GE Healthcare). In addition, tag cleavage was performed by incubating the eluted protein with 0.1 mg of SUMO protease (homemade) and dialyzing overnight at 4 °C against 50 mM Tris/HCl pH 7.5, 150 mM NaCl. The dialyzed sample was loaded again on a 5 mL HisTrap HP column to remove the tag and the SUMO protease. HMFO was eluted in the flow-through fraction and then loaded on a Superdex200 16/60 column (GE Healthcare) equilibrated with 50 mM potassium phosphate buffer pH 7.6. A single and sharp peak was obtained. On the basis of the retention time of HMFO and protein standards of known size, this is consistent with a monomeric homogeneous form of the protein. Fractions were pooled and concentrated with Amicon 30K (Millipore), yielding about 30 mg of pure protein (from 10 g of *E. coli* cells, wet weight).

**Site-Directed Mutagenesis.** To introduce mutations into HMFO, a whole-plasmid PCR was performed. The primers used to introduce the mutations are given in Table S1 of the Supporting Information. The template DNA was cleaved with DpnI (New England BioLabs), and the PCR product was purified afterward using a PCR purification kit (Qiagen). *E. coli* TOP10 cells were transformed with the plasmids, and the introduction of the mutation was confirmed by sequencing.

**Product Formation by Mutant Enzymes V367 and W466 and V367R-W466F.** 2,5-Furandicarboxylic acid (4) generation by wild-type HMFO and the mutant enzymes V367K, V367R, W466F, and W466A or the double mutant enzyme V367R-W466F was assayed by using 2.0 or 20  $\mu$ M enzyme with 5.0 mM 5-hydroxymethylfurfural (1) or 5-formyl-2-furancarboxylic acid (3) in a 100 mM potassium phosphate buffer of pH 7.0 (25 °C, 1000 rpm). The reaction was stopped by heating the mixture at 70 °C. Subsequent centrifugation (5 min at 13000g) was used to remove the denatured enzyme. The products formed were analyzed by HPLC, as described elsewhere.<sup>1</sup>

**Kinetic Analysis.** Steady-state parameters for HMFO wild type and HMFO mutants were obtained by monitoring the conversion of 4-hydroxy-3-methoxybenzyl alcohol (vanillyl alcohol). Formation of the product, 4-hydroxy-3-methoxybenzaldehyde (vanillin), was measured at 340 nm ( $\epsilon_{340} = 14 \text{ mM}^{-1} \text{ cm}^{-1}$ ) using between 0.10 and 4.2  $\mu$ M enzyme, depending on the HMFO variant, while varying the substrate concentration between 0.01 and 40 mM. All kinetic experiments were

performed under atmospheric oxygen conditions. The assay was performed in a 50 mM Tris/HCl buffer pH 7.5 at 25 °C. To determine the steady-state parameters of HMFO V367R, W466F, and V367R-W466F on 5-formyl-2-furancarboxylic acid (3) (TCI Europe), oxygen depletion was measured as described elsewhere.<sup>1</sup> The observed rates were fitted with the Michaelis–Menten kinetics equation,  $v = (k_{\text{cat(app)}}[S]) / ((K_{\text{M(app)}} + [S])$ , or with an equation taking substrate inhibition into account,  $v = (k_{\text{cat(app)}}[S]) / (K_{\text{M(app)}} + [S](1 + [S]/K_{\text{i(app)}}))$ . To determine the  $k_{\text{cat(app)}}/K_{\text{M(app)}}$  values for wild-type HMFO on 5-formyl-2-furancarboxylic acid (3), the oxidation of 0.056 mM up to 4.0 mM substrate was followed at 310 nm ( $\epsilon_{310} = 2.5 \text{ mM}^{-1} \text{ cm}^{-1}$ ) for 60 min in a 50 mM potassium phosphate buffer of pH 8.0. The slope of the linear relation between the observed rate and the concentration of 5-formyl-2-furancarboxylic acid (3) was taken as the  $k_{\text{cat(app)}}/K_{\text{M(app)}}$  value.

**Activity toward Secondary Alcohols.** The activity of HMFO wild-type and mutant enzymes toward the secondary alcohols (*S*)-1-phenylethanol and (*R*)-1-phenylethanol (both Sigma-Aldrich) was assayed by incubating 5.0  $\mu$ M enzyme with 5.0 mM substrate; the reaction was monitored for 50 min. Control reactions without enzyme or without substrate were also performed. Steady-state kinetics of the HMFO W466F and W466A mutants (5  $\mu$ M) were obtained using between 0.05 and 50 mM (*S*)-1-phenylethanol. 1-Phenylethanol conversion was measured by the formation of the product, acetophenone, at 247 nm ( $\epsilon_{247} = 10.8 \text{ mM}^{-1} \text{ cm}^{-1}$ ). Experiments were performed in a 50 mM potassium phosphate buffer of pH 8.0 at 25 °C under atmospheric oxygen concentrations.

**Crystallization and Structure Determination.** Pure HMFO (both wild type and H467A mutant, 10 mg/mL in 50 mM potassium phosphate buffer pH 7.6) was crystallized using the hanging-drop vapor diffusion method by mixing 1.0  $\mu$ L of protein with 1.5  $\mu$ L of a reservoir solution containing 16–22% w/v PEG3350 and 200 mM magnesium formate. Yellow flat crystals grew in 2–5 days at 20 °C. For X-ray data collection crystals were soaked in a cryosolution consisting of 26% w/v PEG3350, 200 mM magnesium formate, and 15% v/v glycerol and flash-cooled in liquid nitrogen. For the structural characterization of enzyme–substrate complexes, crystals were soaked in cryosolutions containing different substrates (5-hydroxymethylfurfural, vanillyl alcohol, (2*E*)-3-phenylprop-2-en-1-ol (cinnamyl alcohol), furan-2,5-dicarbaldehyde, phenylmethanethiol, (4-nitrophenyl)methanethiol, or terephthalaldehyde) using different concentrations depending on compound solubility. Bleaching of the yellow color of the crystal, indicative of flavin reduction, was monitored under the microscope followed by flash-cooling in liquid nitrogen. In the case of the catalytically inactive H467A mutant enzyme, cocrystallization with 10 mM 5-hydroxymethylfurfural was also carried out. X-ray data collection was performed at the beamlines ID23-EH1 (ESRF, Grenoble, France), X06SA (SLS, Villigen, Switzerland), and P13 (DESY-PETRAIII, Hamburg, Germany). Data processing and scaling were performed using MOSFLM<sup>15</sup>

and programs of the CCP4 package.<sup>16</sup> The HMFO structure was initially solved by molecular replacement using the program BALBES,<sup>17</sup> which selected choline oxidase as the best starting model (PDB code 4MJW; 31% sequence identity). Model building and structure analysis were performed by the program COOT,<sup>18</sup> whereas refinement was carried out by REFMAC5.<sup>19</sup> Data collection and refinement statistics are reported in Table S2 in the Supporting Information. Figures were created by CCP4 mg.<sup>20</sup> Atomic coordinates and structure factors were deposited with the Protein Data Bank (codes 4UDP, 4UDQ, and 4UDR).

## RESULTS AND DISCUSSION

Three structures of the enzyme, the wild type in its oxidized and reduced forms and a mutant enzyme (HMFO H467A), were solved at 1.6–1.9 Å resolution (Figure 1A and Figure S1

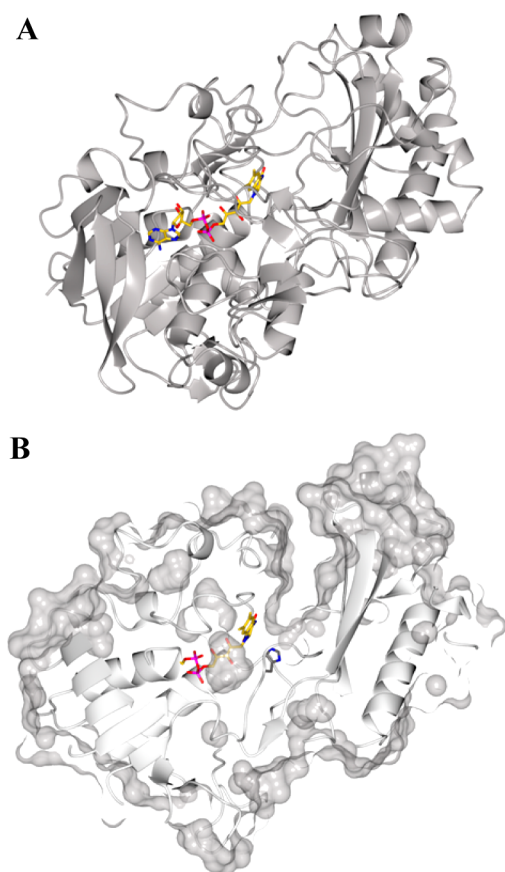


**Figure 1.** Three-dimensional structure of HMFO: (A) ribbon diagram of the overall structure with its FAD cofactor bound (represented with carbon, oxygen, nitrogen, and phosphorus atoms in yellow, red, blue, and magenta, respectively); (B) HMFO surface highlighting the active site cleft that is about 20 Å deep and on average 10 Å large (the representation was front- and back-clipped to make the cleft space visible). In front of the flavin ring the side chain of the conserved His467 is at the bottom of the active site.

and Table S2 in the Supporting Information). Out of the 531 residues of HMFO, only the four N-terminal and two C-terminal amino acids lack clear electron density, whereas loop 326–330 is poorly ordered in the oxidized enzyme. Though being monomeric in solution, the two HMFO molecules present in the asymmetric unit form a dimer that involves a limited interface area with no catalytically relevant regions (less

than 4% of the total protein surface). Comparison with other proteins of the GMC family revealed that choline oxidase,<sup>21</sup> pyridoxine-4-oxidase,<sup>22</sup> and aryl-alcohol oxidase<sup>23</sup> have structural architectures the most similar to that of HMFO (rmsds calculated on the C<sub>α</sub> positions are 2.0, 2.1, and 2.2 Å, respectively), followed by glucose oxidase<sup>24</sup> (rmsd of 2.3 Å) and pyranose-2-oxidase<sup>25</sup> (rmsd of 3.0 Å). Choline oxidase and glucose oxidase have dimeric structures, which, unlike HMFO, are essential for their catalytic activity and involve about 10% of their monomer surface.

The 531 HMFO residues fold into a globular and compact structure organized in two domains: the FAD-binding domain (residues 5–158, 208–307, 372–402, and 466–529), characterized by the typical Rossmann fold topology that embeds the noncovalently bound FAD cofactor, and a smaller cap domain (residues 159–207, 308–371, 403–465) that covers the flavin site. Some oxidases of the GMC family, such as choline oxidase and pyranose-2-oxidase, contain a covalently bound FAD cofactor, linked via a 8 $\alpha$ -N3-histidyl bond. In HMFO, V101 replaces the histidine present in these enzymes. Mutagenesis experiments show that introducing a histidine in HMFO does not result in a covalently bound cofactor and renders the enzyme inactive, possibly because the imidazole ring interferes with proper positioning of the FAD cofactor (Table S3 in the Supporting Information). Only with the double mutant enzyme HMFO F67 V-V101H, designed to leave space for the histidine side chain, was some activity observed, but again, the covalent link was not formed.

At the interface between the FAD and the cap domains of HMFO, a deep and narrow cleft is formed which represents the enzyme active site (Figure 1B). The flavin ring and the side chain of H467 are positioned at the bottom of this cleft. The latter residue is strictly conserved in the oxidases of the GMC family and was shown to be essential for catalysis by functioning as both active site base and H-bond acceptor for the substrate OH group.<sup>1</sup> As anticipated, the H467A mutant enzyme is catalytically almost inactive (activity decrease by >3 orders of magnitude; see Table 1) and the elucidation of its crystal structure showed that the mutation does not result in any conformational change (the overall rmsd for the C<sub>α</sub> atoms with respect to the wild-type protein is 0.39 Å) apart from the binding of three additional water molecules that replace the H467 side chain (Figure S1 in the Supporting Information).

**Table 1.** Steady-State Parameters of the Different HMFO Variants on Vanillyl Alcohol<sup>a</sup>

enzyme	$k_{\text{cat(app)}} \text{ (s}^{-1}\text{)}$	$K_{\text{M(app)}} \text{ (mM)}$	$k_{\text{cat(app)}}/K_{\text{M(app)}} \text{ (s}^{-1}\text{ mM}^{-1}\text{)}$
wild type	21 ± 0.42	0.72 ± 0.066	29
M103A	3.3 ± 0.051	1.8 ± 0.11	1.8
W369A	4.3 ± 0.0063	1.1 ± 0.067	3.9
F434A	15 ± 0.68	1.2 ± 0.23	12
V465A	1.5 ± 0.058	0.92 ± 0.16	1.6
V367K	5.1 ± 0.11	0.29 ± 0.032	18
V367R	6.0 ± 0.12	0.28 ± 0.027	21
W466F	1.7 ± 0.043	0.20 ± 0.027	8.5
W466A	0.75 ± 0.025	1.0 ± 0.15	0.75
H467A <sup>b</sup>	0.0047 ± 0.00023	0.82 ± 0.18	0.0057
N511A	1.0 ± 0.014	2.0 ± 0.10	0.55

<sup>a</sup>Experiments were performed at 25 °C, in 50 mM Tris/HCl buffer of pH 7.5 at atmospheric oxygen concentration. Product formation was measured at 340 nm. <sup>b</sup>Data published elsewhere.<sup>1</sup>

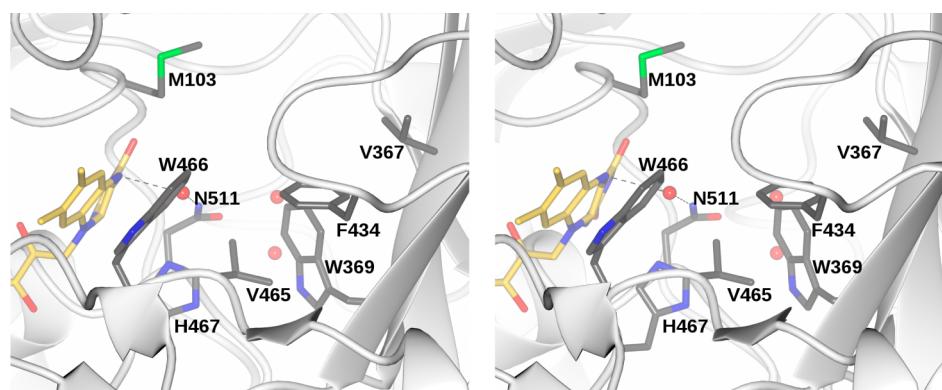


**Figure 2.** Stereoview of the active site of HMFO (reduced state). Residues surrounding the space in front of the flavin ring are shown, including three water molecules (red spheres) that are conserved in all determined HMFO crystal structures (only one is missing in the oxidized enzyme, which may be related to the lower resolution). Color coding is as in Figure 1 (sulfur atoms in green). Hydrogen bonds are represented as dashed lines.

Together with H467, N511 forms a hydrogen-bond dyad for the substrate. N511 is a conserved residue in several GMC type oxidases, and removal of the side chain in the N511A mutant enzyme reduces catalysis, although the effect is much smaller in comparison to that for the H467A mutant enzyme (Table 1). Apart from these two residues, the HMFO active site is quite hydrophobic (Figure 2). Many attempts were made to obtain the structure of HMFO in a complex with either substrate or product by soaking crystals in a mother liquor containing a ligand. By monitoring the bleaching of the yellow color of the crystal (indicating the reduction of the FAD cofactor), we were able to obtain crystals of HMFO in the reduced state. The elucidated structure of the reduced enzyme was essentially indistinguishable from that of the oxidized protein. Moreover, in the substrate reduced enzyme crystals, we could not observe electron density indicating the presence of any ligand. This might be related to the architecture of the HMFO active site cleft, characterized by its free entrance (Figure 1B). Other GMC oxidases also feature a narrow channel for substrate binding, but in these enzymes the active site is more buried and the access to it is often gated by conformational changes of specific loops.<sup>22,23,26,27</sup>

A combination of modeling and mutagenesis experiments was performed to gain insights into the role of several residues in substrate binding. On the basis of the constraints imposed by the position of the  $C_{\alpha}$ -H oxidation site toward the FAD cofactor and the hydroxyl group interaction with H467,<sup>28</sup> we modeled the 5-hydroxymethylfurfural (**1**) molecule in the enzyme active center (Figure 3A). The shape of the cleft constrains the furan ring (as well as the aromatic moiety of vanillyl alcohol, not shown) in a unique conformation, squeezed by the hydrophobic residues surrounding the active site (Figure 2). To investigate this aspect, residues M103, W369, F434, V465, and W466 were mutated to alanine and the steady-state kinetics of the mutant enzymes were studied using vanillyl alcohol as a model substrate (Table 1). The most pronounced effects are observed in the case of the HMFO M103A, W369A, V465A, and W466A mutants. These residues are close to the active site base H467, and their removal creates a large space which likely affects the proper orientation of the substrate with respect to the flavin. In addition, W466 is in close proximity of the flavin ring (Figure 2) and, consistently, removal of this side chain turns out to affect protein stability (Table S4 in the Supporting Information). F434 is farther away

from the oxidation site, and the effect on catalysis of F434A is smaller in comparison to that of the mutant enzymes described above. The overall picture emerging from these experiments is that the active site funnel is designed to create a sterically restrained site that positions the reactive primary alcohol of the substrate in the proper H-bonding environment and geometric relation with the flavin to promote catalysis.

Along this line, we reasoned that some of the created mutant enzymes, though less efficient on primary alcohols, could instead become active on bulkier secondary alcohols as a consequence of an enlarged active site cleft. Consistently, W466F and W466A were found to be active on (*S*)-1-phenylethanol, with W466A performing the best (Table 2). Remarkably, the W466 mutant enzymes are strictly enantioselective, as they have no activity on (*R*)-1-phenylethanol (Table S5 in the Supporting Information), similar to the results for the analogous mutation in the fungal aryl-alcohol oxidase.<sup>29</sup> These data are in full agreement with the structural modeling of 1-phenylethanol in HMFO because the *R* enantiomer would not bind with the  $C_{\alpha}$  hydrogen pointing toward the flavin N5 as requested for oxidation. The *S* enantiomer, on the other hand, would have its methyl group colliding with the W466 side chain, a problem which is overcome by the W466F or W466A mutations (Figure 3B).

The rate-limiting step in the HMFO-catalyzed oxidation of 5-hydroxymethylfurfural (**1**) to 2,5-furandicarboxylic acid (**4**) is the oxidation of 5-formyl-2-furancarboxylic acid (**3**) (Scheme 1).<sup>4</sup> Therefore, increasing the rate of catalysis for this last oxidation step would lead to higher product yields. These thoughts led us to analyze the activity of some of the mutant enzymes toward aldehyde substrates, which have to be in their *gem*-diol form in order to be converted by HMFO. Indeed, both secondary alcohols and *gem*-diols have bulky substituents on the  $\alpha$ -carbon in comparison to primary alcohols. Therefore, although less active on primary alcohols (Table S6 in the Supporting Information), the W466F and W466A mutants were tested against the aldehyde 5-formyl-2-furancarboxylic acid (**3**), both showing increased activity with a noticeable conversion of 49% of 5-formyl-2-furancarboxylic acid (**3**) into 2,5-furandicarboxylic acid (**4**) in 24 h (3 times more than that for the wild type enzyme; Table S6). With these studies W466 was identified as a valuable target site for mutants featuring improved activity on aldehyde substrates by creating a more spacious binding cleft for a *gem*-diol substrate.

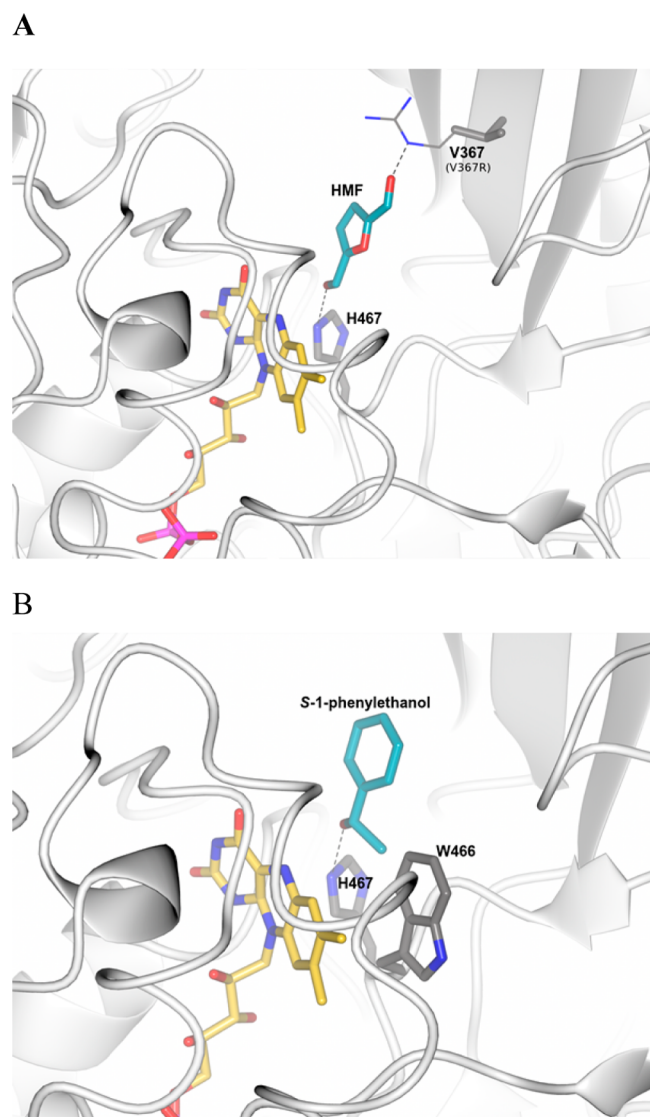


**Figure 3.** Modeling of substrate binding in HMFO active site. (A) Proposed model for the binding of 5-hydroxymethylfurfural substrate (1). The furan ring orientation is constrained by the narrow shape of the cleft, and the substrate  $\alpha$ -carbon is in the proper position to be oxidized by the flavin.<sup>28</sup> The protein atom closest to the substrate hydroxyl group is N $\epsilon$ 2 of His467, which is perfectly positioned to form a H bond with the substrate. The orientation of the His467 imidazole ring was assigned on the basis of a favorable H-bond interaction between its N $\delta$ 1 atom and the neighboring His307 side chain (not shown for clarity). The arginine side chain of the V367R mutant was modeled to show the possible interaction with the substrate, which would provide an explanation for the increased activity of this mutant with 5-formyl-2-furancarboxylic acid (3) (Table 2). (B) Similarly to 5-hydroxymethylfurfural (1), the secondary alcohol (S)-1-phenylethanol was modeled in the HMFO active site. The model is consistent with the biochemical data showing that wild-type HMFO is not able to oxidize this substrate because the substrate methyl group would collide with the W466 side chain. According to the model, the smallest distance between the methyl group of (S)-1-phenylethanol and W466 is 2.3 Å.

Both furanic and phenylic substrates with a negatively charged carboxylic acid on the para position are much less efficiently converted than their noncharged analogues.<sup>1,4</sup> This poor activity of wild-type HMFO toward, for instance, 5-formyl-2-furancarboxylic acid (3) is likely due to a high  $K_{M(\text{app})}$

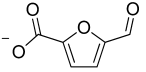
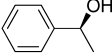
value (Table 2). Similar results were described recently for aryl-alcohol oxidase. This enzyme cannot perform the three oxidations required to form 2,5-furandicarboxylic acid (4) from 5-hydroxymethylfurfural (1), as it is not active toward 5-formyl-2-furancarboxylic acid (3).<sup>30</sup> To improve the activity of HMFO for 5-formyl-2-furancarboxylic acid (3), V367 represents a candidate for mutagenesis (see Figure 3A). Two HMFO mutants, V367 K and V367R, were produced and characterized. It was gratifying to observe that both enzyme variants showed significantly improved activity toward 5-formyl-2-furancarboxylic acid (3) (Table S6). In particular, V367R is able to form 97% of 2,5-furandicarboxylic acid (4) in 6 h, whereas the wild-type enzyme needs 24 h to reach 92% conversion. This can also be seen from the amounts of catalyst needed to obtain 50% conversion: the V367R mutant enzyme outperforms the wild-type protein by reaching similar product quantities in 12 h with 10 times less biocatalyst (Table S6). Similar results are obtained when the entire reaction is tested: i.e., using 5-hydroxymethylfurfural (1) as initial substrate (Table S6). Clearly, HMFO V367R results in a better 5-hydroxymethylfurfural (1) to 2,5-furandicarboxylic acid (4) conversion ( $\sim$ 3-fold higher). These data demonstrate that the introduction of a positive charge at this side of the active site increases the activity toward 5-formyl-2-furancarboxylic acid (3) by helping to position the substrate.

These mutagenesis experiments identified W466 as the site for mutation-increasing activities on the aldehyde 5-formyl-2-furancarboxylic acid (3) and V367 as a site for improving the activity on carboxylic acid containing substrates. A logical continuation was to evaluate the effect of the combined mutations. The V367R-W466F double mutant was constructed and tested for its activity toward 5-formyl-2-furancarboxylic acid (3). The double mutant enzyme has an almost 10-fold higher  $k_{\text{cat}(\text{app})}$  value in comparison to those for the individual single mutant enzymes and also the lowest  $K_{M(\text{app})}$  value (Table 2), resulting in a catalytic efficiency ( $k_{\text{cat}}/K_M$ ) for 5-formyl-2-furancarboxylic acid (3) that is over 1000-fold higher than that for wild-type HMFO. HPLC analysis confirms the double mutant is superior to both the single mutants and wild-type HMFO for the formation of 2,5-furandicarboxylic acid (4) (Table S6 in the Supporting Information). Moreover, the double mutant displayed enhanced efficiency in the overall conversion of 5-hydroxymethylfurfural (1) to 2,5-furandicarboxylic acid (4), a feature of self-evident relevance for the biotechnological applications of the enzyme.

## CONCLUSIONS

An intriguing aspect of HMFO is its dual character of being very precise in the oxidation of primary alcohols (i.e., devoid of any activity on secondary alcohols) and at the same time so promiscuous in converting a broad range of primary alcohols. At the heart of this feature is an active-site cleft which provides an essential H-bonding anchoring point that activates the substrate and positions the substrate  $\alpha$  carbon in direct contact with the flavin. The crystal structure shows that a constellation of mostly hydrophobic amino acids shapes the active site cleft to make it selective for aromatic and aliphatic primary alcohols. This active site architecture is amenable to protein engineering to design biocatalysts with enhanced activities toward substrates with varying bulkiness and electrostatic properties. In particular, it was possible to identify mutant enzymes that are active on secondary alcohols, with the added value that their enantioselectivity can be used for kinetic resolution of chiral secondary alcohols.<sup>31–33</sup> Equally valuable, mutant enzymes

Table 2. Steady-State Parameters of the Engineered HMFO Variants<sup>a</sup>

Enzyme	$k_{\text{cat (app)}} \text{ (s}^{-1}\text{)}$	$K_{\text{M (app)}} \text{ (mM)}$	$k_{\text{cat (app)}}/K_{\text{M (app)}} \text{ (s}^{-1} \text{ mM}^{-1}\text{)}$
wild type	n.s. <sup>b</sup>	> 4.0	0.0005
V367R <sup>c</sup>		1.4	0.041
W466F		3.0	0.026
V367R-W466F <sup>c</sup>		0.21	2.2
wild type	n.d. <sup>d</sup>	n.d.	n.d.
W466A		20	$0.55 \cdot 10^{-3}$
W466F		98	$0.10 \cdot 10^{-3}$

<sup>a</sup>The activity of HMFO variants toward 5-formyl-2-furancarboxylic acid (3) was measured using O<sub>2</sub> depletion, whereas the activity toward (S)-1-phenylethanol was measured by the formation of product at 247 nm ( $\epsilon_{247} = 10.8 \text{ mM}^{-1} \text{ cm}^{-1}$ ) in a 50 mM potassium phosphate buffer of pH 8.0 at 25 °C at atmospheric oxygen concentration. <sup>b</sup>n.s. = no saturation. The activity of HMFO under saturated substrate conditions could not be measured, preventing estimation of the  $k_{\text{cat (app)}}$  value. The  $k_{\text{cat (app)}}/K_{\text{M (app)}}$  value for wild-type HMFO was determined by measuring the decrease of 5-formyl-2-furancarboxylic acid (3) ( $\epsilon_{310} = 3.7 \text{ mM}^{-1} \text{ cm}^{-1}$ ) at a low concentration of 5-formyl-2-furancarboxylic acid (3) ( $\leq 4.0 \text{ mM}$ ), where the linear relation between the rates ( $\text{s}^{-1}$ ) and the substrate concentration (mM) represents  $k_{\text{cat (app)}}/K_{\text{M (app)}}$ . <sup>c</sup>Both HMFO V367R and V367R-W466F show substrate inhibition, with  $K_{\text{i (app)}}$  values of 76 and 7.3 mM, respectively. <sup>d</sup>n.d. = not detectable. No activity can be detected toward (S)-1-phenylethanol using wild-type HMFO.

were created with increased activity toward the intermediates formed during the multistep HMFO-mediated production of 2,5-furandicarboxylic acid (4). These properties culminate in a double mutant that combines the best of these individual mutant enzymes, having the highest turnover number and affinity for 5-formyl-2-furancarboxylic acid (3), leading to the highest 2,5-furandicarboxylic acid (4) yield. All these findings will guide further investigations on HMFO catalytic activities and will be valuable for industries focused on green chemistry approaches for biobased plastics production.

## ■ ASSOCIATED CONTENT

### ■ Supporting Information

The following file is available free of charge on the ACS Publications website at DOI: 10.1021/cs5b0003a.

Primers used for the generation of the mutant enzymes (Table S1), electron density showing the H467A mutation in the crystal structure (Figure S1), data collection and refinement statistics for HMFO, oxidized and reduced, and HMFO H467A (Table S2), steady-state kinetics of HMFO V101H mutants (Table S3), spectral properties and apparent melting temperatures of all HMFO mutants (Table S4), activity toward secondary alcohols (Table S5), and data on 5-hydroxymethylfurfural (1) and 5-formyl-2-furancarboxylic acid (3) conversion using different experimental conditions and HMFO mutant enzymes (Table S6) (PDF)

## ■ AUTHOR INFORMATION

### Corresponding Authors

\*E-mail for M.W.F.: m.w.fraaije@rug.nl.

\*E-mail for A.M.: andrea.mattevi@unipv.it.

### Author Contributions

<sup>§</sup>These authors contributed equally.

### Notes

The authors declare no competing financial interest.

## ■ ACKNOWLEDGMENTS

This work was carried out within the BE-Basic R&D Program, for which an FES subsidy was granted from the Dutch Ministry of Economic Affairs, Agriculture, and Innovation (EL&I). We thank the European Synchrotron Radiation Facility (ESRF), the Swiss Light Source (SLS), and the Deutsches Elektronen-Synchrotron (DESY-PETRAIII) for providing beam time and assistance. We thank also the BioStruct-X program (projects nos. 5275 and 7551) for funding synchrotron trips.

## ■ ABBREVIATIONS

HMFO, 5-hydroxymethylfurfural oxidase; GMC, glucose-methanol-choline; FAD, flavin adenine dinucleotide

## ■ REFERENCES

- (1) Dijkman, W. P.; Fraaije, M. W. *Appl. Environ. Microbiol.* **2014**, *80*, 1082–1090.
- (2) Jong, E. de; Dam, M. A.; Sipos, G. J.; Gruter, M. In *Biobased Monomers, Polymers, and Materials*; American Chemical Society: Washington, DC, 2012; pp 1–13.
- (3) Kamm, B. *Angew. Chem., Int. Ed. Engl.* **2007**, *46*, 5056–5058.
- (4) Dijkman, W. P.; Groothuis, D. E.; Fraaije, M. W. *Angew. Chem., Int. Ed. Engl.* **2014**, *53*, 6515–6518.
- (5) Romero, E.; Gadda, G. *Biomol. Concepts* **2014**, *5*, 299–318.
- (6) Smitherman, C. L.; Rungsririyachai, K.; Germann, M. W.; Gadda, G. *Biochemistry* **2015**, *54*, 413–421.
- (7) Mugo, A. N.; Kobayashi, J.; Yamasaki, T.; Mikami, B.; Ohnishi, K.; Yoshikane, Y.; Yagi, T. *Biochim. Biophys. Acta* **2013**, *1834*, 953–963.
- (8) Yue, Q. K.; Kass, I. J.; Sampson, N. S.; Vrieling, A. *Biochemistry* **1999**, *38*, 4277–4286.
- (9) Wongnate, T.; Sucharitakul, J.; Chaiyen, P. *Chembiochem* **2011**, *12*, 2577–2586.
- (10) Hernández-Ortega, A.; Lucas, F.; Ferreira, P.; Medina, M.; Guallar, V.; Martínez, A. T. *Biochemistry* **2012**, *51*, 6595–6608.
- (11) Fan, F.; Gadda, G. *J. Am. Chem. Soc.* **2005**, *127*, 2067–2074.
- (12) Hernández-Ortega, A.; Borrelli, K.; Ferreira, P.; Medina, M.; Martínez, A. T.; Guallar, V. *Biochem. J.* **2011**, *436*, 341–350.
- (13) Wongnate, T.; Chaiyen, P. *FEBS J.* **2013**, *280*, 3009–3027.

- (14) Ewing, T. A.; Dijkman, W. P.; Vervoort, J. M.; Fraaije, M. W.; van Berkel, W. J. H. *Angew. Chem., Int. Ed. Engl.* **2014**, *53*, 13206–13209.
- (15) Battye, T. G. G.; Kontogiannis, L.; Johnson, O.; Powell, H. R.; Leslie, A. G. W. *Acta Crystallogr. D. Biol. Crystallogr.* **2011**, *67*, 271–281.
- (16) Winn, M. D.; Ballard, C. C.; Cowtan, K. D.; Dodson, E. J.; Emsley, P.; Evans, P. R.; Keegan, R. M.; Krissinel, E. B.; Leslie, A. G. W.; McCoy, A.; McNicholas, S. J.; Murshudov, G. N.; Pannu, N. S.; Potterton, E. A.; Powell, H. R.; Read, R. J.; Vagin, A.; Wilson, K. S. *Acta Crystallogr. D. Biol. Crystallogr.* **2011**, *67*, 235–242.
- (17) Long, F.; Vagin, A. A.; Young, P.; Murshudov, G. N. *Acta Crystallogr. D. Biol. Crystallogr.* **2008**, *64*, 125–132.
- (18) Emsley, P.; Cowtan, K. D. *Acta Crystallogr. D. Biol. Crystallogr.* **2004**, *60*, 2126–2132.
- (19) Murshudov, G. N.; Vagin, A. A.; Dodson, E. J. *Acta Crystallogr. D. Biol. Crystallogr.* **1997**, *53*, 240–255.
- (20) McNicholas, S.; Potterton, E.; Wilson, K. S.; Noble, M. E. M. *Acta Crystallogr. D. Biol. Crystallogr.* **2011**, *67*, 386–394.
- (21) Quaye, O.; Cowins, S.; Gadda, G. J. *Biol. Chem.* **2009**, *284*, 16990–16997.
- (22) Mugo, A. N.; Kobayashi, J.; Mikami, B.; Ohnishi, K.; Yagi, T. *Acta Crystallogr. Sect. F. Struct. Biol. Cryst. Commun.* **2012**, *68*, 66–68.
- (23) Fernández, I. S.; Ruíz-Dueñas, F. J.; Santillana, E.; Ferreira, P.; Martínez, M. J.; Martínez, A. T.; Romero, A. *Acta Crystallogr. D. Biol. Crystallogr.* **2009**, *65*, 1196–1205.
- (24) Hecht, H.-J.; Kalisz, H. M.; Hendle, J.; Schmid, R. D.; Schomburg, D. *J. Mol. Biol.* **1993**, *229*, 153–172.
- (25) Hallberg, B. M.; Leitner, C.; Haltrich, D.; Divne, C. *J. Mol. Biol.* **2004**, *341*, 781–796.
- (26) Spadiut, O.; Tan, T.-C.; Pisanelli, I.; Haltrich, D.; Divne, C. *FEBS J.* **2010**, *277*, 2892–2909.
- (27) Quaye, O.; Lountos, G. T.; Fan, F.; Orville, A. M.; Gadda, G. *Biochemistry* **2008**, *47*, 243–256.
- (28) Fraaije, M. W.; Mattevi, A. *Trends Biochem. Sci.* **2000**, *25*, 126–132.
- (29) Hernández-Ortega, A.; Ferreira, P.; Merino, P.; Medina, M.; Guallar, V.; Martínez, A. T. *Chembiochem* **2012**, *13*, 427–435.
- (30) Carro, J.; Ferreira, P.; Rodríguez, L.; Prieto, A.; Serrano, A.; Balcells, B.; Ardá, A.; Jiménez-Barbero, J.; Gutiérrez, A.; Ullrich, R.; Hofrichter, M.; Martínez, A. T. *FEBS J.* **2014**, DOI: 10.1111/febs.13177.
- (31) Turner, N. J. *Chem. Rev.* **2011**, *111*, 4073–4087.
- (32) O'Reilly, E.; Iglesias, C.; Ghislieri, D.; Hopwood, J.; Galman, J. L.; Lloyd, R. C.; Turner, N. J. *Angew. Chem., Int. Ed. Engl.* **2014**, *53*, 2447–2450.
- (33) Escalettes, F.; Turner, N. J. *Chembiochem* **2008**, *9*, 857–860.